RESEARCH ARTICLE
PLANETARY SCIENCES

Earth and Planetary Physics
4: 17–22, 2020
doi: 10.26464/epp2020008

Photoelectron pitch angle distribution near Mars and implications on cross terminator magnetic field connectivity

YuTian Cao[1,2], Jun Cui[3,4*], XiaoShu Wu[1,4], and JiaHao Zhong[3]

[1]Key Laboratory of Lunar and Deep Space Exploration, National Astronomical Observatories, Chinese Academy of Sciences, Beijing 100012, China;

[2]School of Astronomy and Space Sciences, University of Chinese Academy of Sciences, Beijing 100049, China;

[3]School of Atmospheric Sciences, Sun Yat-sen University, Zhuhai Guangdong 519082, China;

[4]Center for Excellence in Comparative Planetology, Chinese Academy of Sciences, Hefei 230026, China

Key Points:

- An analysis is conducted focusing on the pitch angle distribution of energetic electrons at 22–27 eV at Mars
- Two cases of dayside photoelectrons with anisotropic pitch angle distribution are proposed
- These anisotropic photoelectron observations on the dayside indicate the presence of cross terminator magnetic field topology

Citation: Cao, Y. T., Cui, J., Wu, X. S., and Zhong, J. H. (2020). Photoelectron pitch angle distribution near Mars and implications on cross terminator magnetic field connectivity. *Earth Planet. Phys.*, *4*(1), 17–22. http://doi.org/10.26464/epp2020008

Abstract: The photoelectron peak at 22–27 eV, a distinctive feature of the energetic electron distribution in the dayside Martian ionosphere, is a useful diagnostic of solar extreme ultraviolet (EUV) and X-ray ionization as well as of large-scale transport along magnetic field lines. In this work, we analyze the pitch angle distribution (PAD) of energetic electrons at 22–27 eV measured during several representative Mars Atmosphere and Volatile Evolution (MAVEN) orbits, based on the electron spectra gathered by MAVEN's Solar Wind Electron Analyzer (SWEA) instrument. On the dayside, most photoelectron spectra show an isotropic PAD as is expected from production via solar EUV/X-ray ionization. The photoelectron spectra occasionally observed on the nightside show instead a strongly anisotropic PAD, indicative of cross-terminator transport along ambient magnetic field lines. This would in turn predict the presence of dayside photoelectrons, also with a strongly anisotropic PAD, which was indeed revealed in SWEA data. Comparison with magnetic field measurements made by the MAVEN Magnetometer suggests that on average the photoelectrons with anisotropic PAD stream away from Mars on the dayside and towards Mars on the nightside, further supporting the scenario of day-to-night transport. On both sides, anisotropic photoelectrons tend to be observed above the photoelectron exobase at ~160 km where photoelectron transport dominates over local production and energy degradation.

Keywords: Mars; MAVEN; photoelectron; Day-to-night transport

1. Introduction

Photoionization is the dominant source of ionization in dayside planetary upper atmospheres (Withers, 2009). Photoelectrons, as an important population of ionospheric plasma, can be produced by solar Extreme Ultraviolet (EUV) and X-ray ionization of various molecules in the ambient atmosphere (e.g. Coates et al., 2011). The He II 30.4 nm line is one of the most intense EUV lines in the solar spectrum; it produces peaks in the photoelectron energy distributions observed on various Solar System bodies, at fixed energies that depend on the dominant constituents in each body's upper atmosphere. At Mars, photoelectrons with energy peaks at ~22 eV and ~27 eV are observed due to the ionization of CO_2 and O (e.g. Mantas and Hanson, 1979; Frahm et al., 2006; Sakai et al., 2015; Peterson et al., 2016). These photoelectrons are typically magnetized with guiding center motions along the ambient magnetic field lines, implying that photoelectrons are a useful diagnostic of the magnetic field topology near Mars (e.g. Coates et al., 2011).

Recently, several studies inferring the magnetic topology at Mars have been conducted, based on energetic electron measurements made by the Solar Wind Electron Analyzer (SWEA) onboard the Mars Atmosphere and Volatile Evolution (MAVEN) space craft (e.g. Xu SS et al., 2016, 2017a, b, 2019; Weber et al., 2017). Xu SS et al. (2019) combined two independent methods — one based on the pitch angle distribution (PAD) and the other on the energy distribution of suprathermal electrons — to identify seven magnetic topologies in the Martian ionosphere. In terms of PAD, these studies focus primarily on energetic electrons at 100–300 eV, which effectively targets the shocked incoming solar wind (SW) (Weber et al., 2017). The SW electron precipitation, as part of the ionizing source in the dayside ionosphere, is thought to be the dominant source of ionization in the deep nightside, where photoionization is switched off (e.g. Verigin et al., 1991; Fowler et al.,

Correspondence to: J. Cui, cuijun7@mail.sysu.edu.cn
Received 06 NOV 2019; Accepted 28 NOV 2019.
Accepted article online 13 DEC 2019.
©2020 by Earth and Planetary Physics.

2015). Below 140 km, electron precipitation is proposed to be able fully to maintain the nightside Martian ionosphere with no need for contributions from other sources (Cui J et al., 2019). The magnetic topology identification based on these SW electrons improves our understanding of the effects of magnetic fields on electron precipitation (e.g. Lillis et al., 2009, 2011, 2018; Lillis and Brain, 2013).

In addition to electron impact ionization, day-to-night plasma transport also serves as an important mechanism supporting the nightside Martian ionosphere, especially near the terminator (e.g. Zhang et al., 1990; Fox et al., 1993; Němec et al., 2010; Duru et al., 2011; Withers et al., 2012; Cao YT et al., 2019). A similar process is known to occur on other terrestrial planets, such as Venus (Knudsen et al., 1980; Spenner et al., 1981; Knudsen and Miller, 1992) and Titan (Cui J et al., 2009, 2010). By analyzing data from the Mars Express (MEx) Mars Advanced Radar for Subsurface and Ionospheric Sounding (MARSIS), Cui J et al. (2015) reached the conclusion that, for a time duration of 5000 s after terminator crossing, day-to-night transport dominates over SW electron precipitation. Photoionization is the only source of the spectral peaks in the photoelectron energy distribution, unlike the production of thermal ionospheric plasma, which occurs via either photoionization on the dayside or SW electron impact ionization on the nightside. Such a distinction implies that the photoelectron peak at 22–27 eV observed near Mars is a superior tracer of day-to-night plasma transport. This observation motivates the main objective of the present study: we analyze the variation of the photoelectron PAD along the cross-terminator trajectories during several representative MAVEN orbits.

2. Data Description

The primary data product required for the purpose of this study is the differential energetic electron intensity measurements made by the SWEA instrument onboard MAVEN (Mitchell et al., 2016). The SWEA is a symmetric hemispheric electrostatic analyzer that measures the suprathermal electron intensity as a function of energy per charge, covering the energy range of 3–4.6 keV with a resolution of 17% ($\Delta E/E$), and also as a function of the direction of arrival, covering a field of view (FOV) of 360° × 120° of which 8% is blocked by the spacecraft body. Due to the limited energy resolution, the SWEA cannot distinguish the photoelectron energy peaks at 22 eV and 27 eV. The photoelectron PAD is determined by combining SWEA data and magnetic field data measured by the MAVEN Magnetometer (MAG) (Connerney et al., 2015).

3. The Variation of Photoelectron PAD

We start with the variation of the electron energy spectra measured during MAVEN orbit #1817 on 5 September 2015 in the fourth Deep Dip campaign. During this orbit, the spacecraft flew from the dayside to the nightside relative to Mars with the periapsis located near the terminator in the southern hemisphere. The SWEA measurements obtained during part of this orbit are shown in Figure 1. In panels (a) and (b), we present the SWEA spectra parallel and anti-parallel to the ambient magnetic field direction, defined as within the pitch angle ranges of 0°–10° and 170°–180°, respectively. For reference, we also display in panels (c) and (d) the intensities of the total magnetic field and its three components measured by the MAG in local coordinates (with *X*, *Y*, and *Z* pointing towards local north, local east, and vertically downward), as well as the height and solar zenith angle (SZA) at the spacecraft location. The dashed line in panel (c) gives the variation of the magnetic field elevation angle along the spacecraft trajectory with 0° representing a strictly horizontal magnetic field relative to the surface of Mars. We further present in the top panels of Figure 2 the fan plots of the electron energy distribution averaged over four sweeps at several locations along the spacecraft trajectory and along all pitch angles. These locations are indicated by the vertical dashed lines in Figure 1. In the bottom panels of Figure 2, we compare the SWEA spectra for three pitch angle ranges along the parallel, anti-parallel, and vertical directions relative to the ambient magnetic fields.

From 01:01:16 UT (universal time) to 01:04:48 UT in Figure 1, the height of the spacecraft declined continuously towards a periapsis altitude of 123 km, while the SZA increased from 71° to 85°. This was a period during which the discrete photoelectron energy peak at 22–27 eV was seen persistently in both the parallel and anti-parallel directions. A closer look at the dayside electron energy spectra reveals that the photoelectron intensities at 22–27 eV along different directions are overall comparable, implying that the dayside photoelectron PAD tends to be isotropic, which is an expected result of isotropic photoelectron production via solar EUV/X-ray ionization. The isotropy of the photoelectron PAD can be seen more clearly in Figure 2b, where the difference in photoelectron intensity among the displayed directions is no more than 20% at all energies of interest here.

After 01:06:00 UT in Figure 1, the MAVEN spacecraft passed the terminator and entered into the nightside of Mars. The SWEA measurements generally showed no signature of the photoelectron peak, which was instead manifested as isolated periods of suprathermal electron depletion, as reported by Steckiewicz et al. (2015, 2017). Despite this, the photoelectron energy peak could occasionally be seen in the deep nightside of Mars where the He II line radiation was expected to be fully attenuated and no local source of photoelectron production was available. Such a signature was clearly seen at 01:10:56 UT in Figure 1 and, more interestingly, the signature was restricted to the direction parallel to the ambient magnetic field line but not in the opposite direction. This characteristic is further demonstrated by the full photoelectron PAD in Figure 2c where a comparison of the SWEA spectra between different directions reveals the parallel intensity to be a factor of 4 higher than the anti-parallel intensity. The presence of photoelectrons in the deep nightside has already been noticed by Xu SS et al. (2016), as evidence of day-to-night transport facilitated by cross-terminator magnetic field connectivity, but here such a conclusion is further augmented by our analysis of the photoelectron PAD on the nightside, which is fully consistent with the transport scenario.

If the above scenario is correct, then one would naturally expect to observe dayside photoelectrons streaming away from Mars and characterized by a strongly anisotropic PAD. Figure 1 shows such a situation, in SWEA measurements at 01:01:29 UT for an SZA of 72°. More specifically, Figure 2a reveals that the anti-parallel pho-

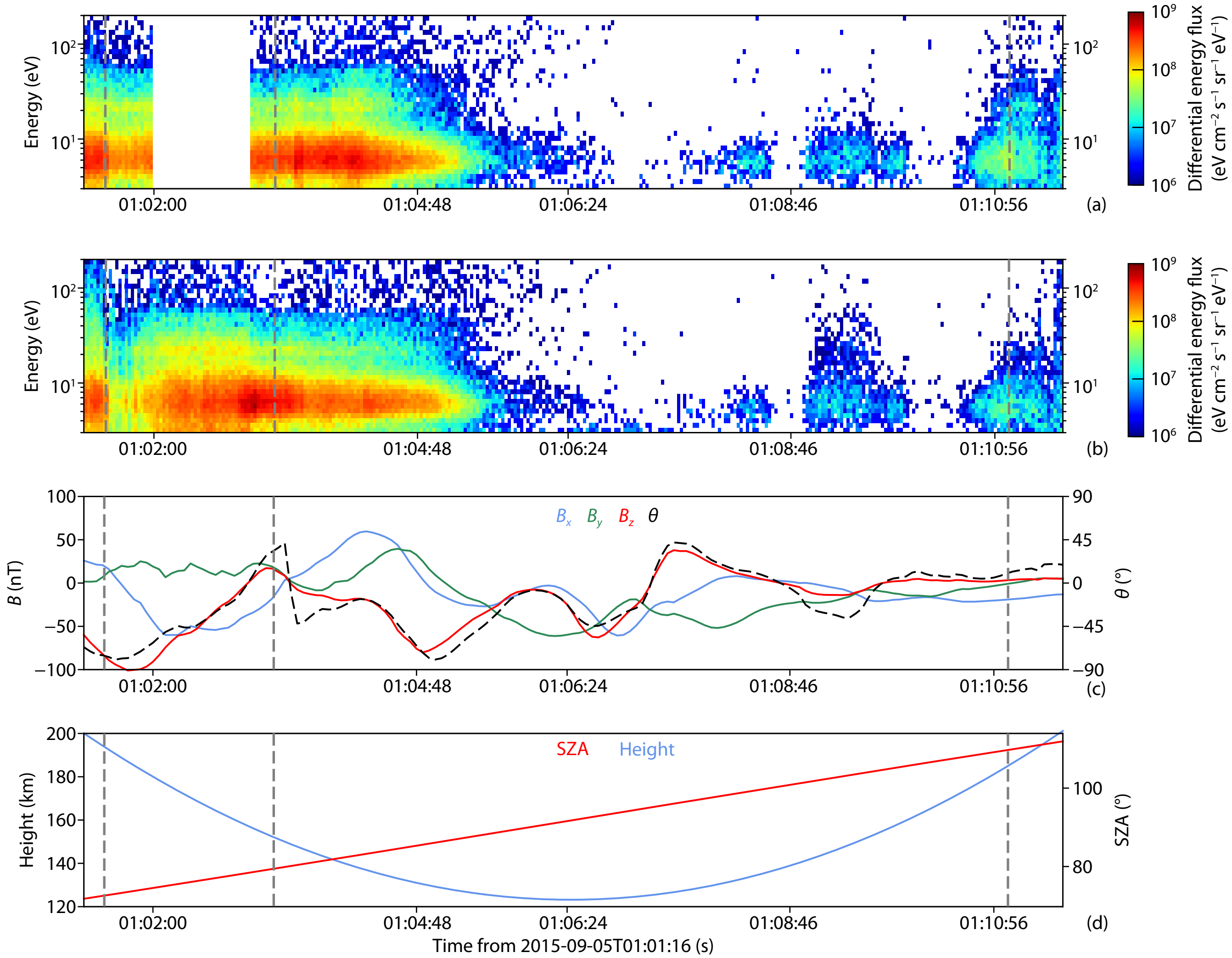

Figure 1. (a) The SWEA electron energy spectra along the direction parallel to the ambient magnetic fields during MAVEN orbit #1817 on 5 September 2015; (b) Similar to panel (a) along the direction anti-parallel to the ambient magnetic fields; (c) The intensities of the total magnetic field and its three components measured by the MAG in local coordinates, as well as the respective magnetic elevation angle; (d) The height and SZA at the spacecraft location.

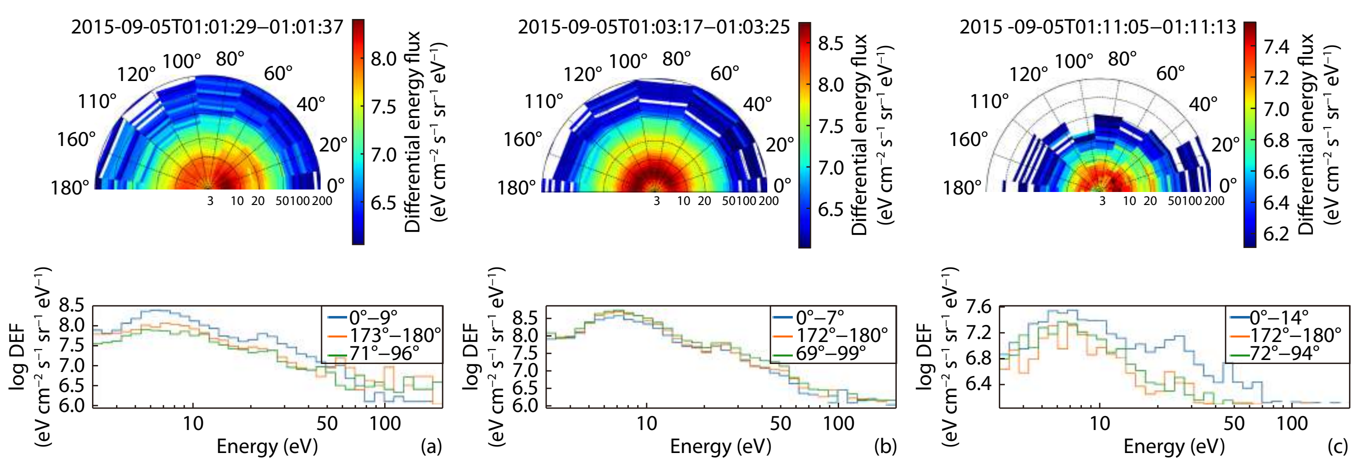

Figure 2. (Top) Fan plots of the electron energy distribution averaged over four sweeps at several locations along the spacecraft trajectory during MAVEN orbit #1817 and along all pitch angles. These locations are indicated by the vertical dashed lines in Figure 1. (Bottom) The SWEA spectra for three pitch angle ranges along the parallel, anti-parallel, and vertical directions relative to the ambient magnetic fields.

toelectron intensity was reduced by more than 60% compared to the parallel intensity. Since the local magnetic field was in the vertically upward direction, as shown in Figure 1c, the observed anisotropic PAD suggests that, on average, photoelectrons were indeed streaming away from Mars. The possibility that the anisotropic PAD could be indicative of photoelectron escape along open magnetic field lines could be ruled out; if that were the case, the SWEA would not observe photoelectrons in the anti-parallel direction (Xu SS et al., 2017a, 2019). The data are consistent with the following two possibilities: that the photoelectrons were moving along closed magnetic field lines, either with both footprints on the dayside of Mars or with one footprint on the dayside and the other footprint on the nightside. The large difference in photoelectron intensity observed between parallel and anti-parallel, however, suggests that the latter is more likely to represent the real situation (Xu SS et al., 2019).

In Figure 3, we show a further example, for MAVEN orbit #5344 on 2 July 2017, during which the signature of anisotropic photoelectron PAD was more prominent. This orbit occurred in the nominal mission phase with a periapsis altitude of 157 km in the northern hemisphere of Mars. Below 200 km, the spacecraft was fully on the dayside at large SZA; accordingly, the entire SWEA spectra shows clear signatures of photoelectron peak at 22–27 eV in all directions within the instrument FOV. The photoelectron PAD is roughly isotropic in the middle of Figure 3, which corresponds to regions with a relatively density ambient atmosphere where local production of photoelectrons is dominated by solar EUV/X-ray radiation. The degree of anisotropy increases with increasing height over both the inbound and outbound portions of the orbit, indicative of the importance of photoelectron transport; but now the photoelectron intensity along the direction anti-parallel to the magnetic field is substantially stronger than the intensity along the parallel direction. The MAG measurements displayed in Figure 3c suggest that the ambient magnetic fields were in the slanted and downward direction over most of the MAVEN trajectory during this orbit, from which we conclude that the observed dayside photoelectrons were also streaming away from Mars, as was observed also during orbit #1817 at 01:01:29 UT.

4. Discussion and Concluding Remarks

Day-to-night transport is an important mechanism maintaining the nightside Martian ionosphere (e.g. Withers et al., 2012; Cui J et al., 2015; Cao YT et al., 2019). Photoelectrons, characterized by distinctive spectral peaks at 22–27 eV, provide a better tracer of such a process than thermal electrons because the former could by

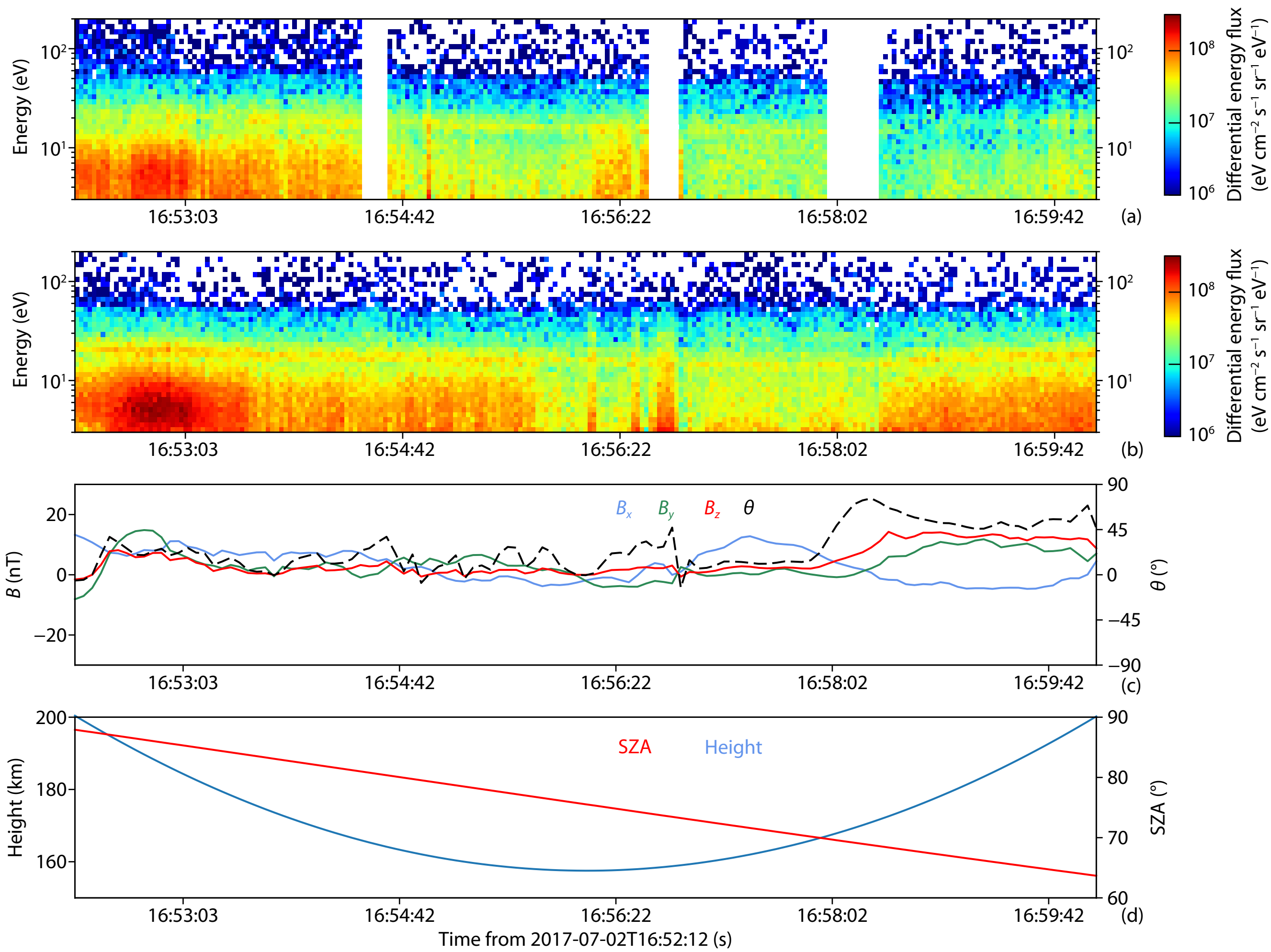

Figure 3. Same as in Figure 1 except for MAVEN orbit #5433.

produced only by photoionization, whereas the latter could be produced by both photoionization and electron impact ionization (e.g. Verigin et al., 1991; Fowler et al., 2015; Cui J et al., 2019).

In this study, we present the energetic electron spectra measured by the SWEA in the Martian ionosphere below 200 km during MAVEN orbit #1817 on 5 September 2015 that crossed the terminator. On the dayside, the majority of the observed photoelectrons presented a near isotropic PAD as expected by local production via solar EUV/X-ray ionization. Photoelectrons could occasionally be observed in the deep nightside, but these photoelectrons were characterized by a strongly anisotropic PAD, consistent with the scenario of photoelectron transport along closed magnetic field lines connecting both the dayside and nightside of Mars (e.g. Xu SS et al., 2016, 2017a, 2019). Such a scenario would also predict the presence of dayside photoelectrons that on average stream away from Mars. This was indeed revealed by SWEA measurements made during MAVEN orbit #1817, which exhibit a remarkable difference in photoelectron intensity between different field-aligned directions (parallel and anti-parallel), though not as much as on the nightside. A similar feature was more prominently recorded during MAVEN orbit #5344, over a more extended region of the dayside Martian upper atmosphere. On both the dayside and nightside, regions with clearly anisotropic photoelectron PAD tended to be located above the photoelectron exobase, ~160 km on Mars (Xu SS et al., 2016), where photoelectron transport dominates over local production and energy degradation (e.g. Wu XS et al., 2019).

The variation of the photoelectron PAD reported here is consistent with a scenario in which the photoelectrons are able to bounce between the dayside and nightside ionospheres along cross-terminator magnetic field lines because of conservation of the first adiabatic invariant and the magnetic mirror effect. During such a process, a portion of the photoelectrons might be lost due to collisions with ambient neutrals, and then not replenished on the nightside. If so, we not expect to see more photoelectrons flowing towards the nightside than those bouncing back towards the dayside. The above scenario is fully compatible with the observation of enhanced photoelectron intensity streaming away from Mars on the dayside and streaming towards Mars on the nightside. The anisotropic PAD of energetic electrons has been reported in some previous works but exclusively referring to energies above 100 eV, a region in which SW electrons would be likely to dominate photoelectrons (e.g. Weber et al., 2017; Xu SS et al., 2019). Constraining the PAD analysis to electrons at 22–27 eV as we do here is likely to provide an ideal clue to the role of day-to-night transport in maintaining the nightside Martian ionosphere.

Acknowledgments

This work is supported by the pre-research project on Civil Aerospace Technologies No. D020105 funded by China's National Space Administration. The authors also acknowledge support from the National Natural Science Foundation of China through grants 41525015, 41774186, and 41904154. The SWEA data used in the present study are publicly available at the MAVEN Science Data Center (https://lasp.colorado.edu/maven/sdc/public/).

References

Cao, Y. T., Cui, J., Wu, X. S., Guo, J. P., and Wei, Y. (2019). Structural variability of the Nightside Martian ionosphere near the terminator: Implications on plasma sources. *J. Geophys. Res. Planets*, *124*(6), 1495–1511. https://doi.org/10.1029/2019JE005970

Coates, A. J., Tsang, S. M. E., Wellbrock, A., Frahm, R. A., Winningham, J. D., Barabash, S., Lundin, R., Young, D. T., and Crary, F. J. (2011). Ionospheric photoelectrons: Comparing Venus, Earth, Mars and Titan. *Planet. Space Sci.*, *59*(10), 1019–1027. https://doi.org/10.1016/j.pss.2010.07.016

Connerney, J. E. P., Espley, J., Lawton, P., Murphy, S., Odom, J., Oliversen, R., and Sheppard, D. (2015). The MAVEN magnetic field investigation. *Space Sci. Rev.*, *195*(1-4), 257–291. https://doi.org/10.1007/s11214-015-0169-4

Cui, J., Galand, M., Yelle, R. V., Vuitton, V., Wahlund, J. E., Lavvas, P. P., Müller-Wodarg, I. C. F., Cravens, T. E., Kasprzak, W. T., and Waite, Jr. J. H. (2009). Diurnal variations of Titan's ionosphere. *J. Geophys. Res. Space Phys.*, *114*(A6), A06310. https://doi.org/10.1029/2009JA014228

Cui, J., Galand, M., Yelle, R. V., Wahlund, J. E., Ågren, K., Waite, Jr. J. H., and Dougherty, M. K. (2010). Ion transport in Titan's upper atmosphere. *J. Geophys. Res. Space Phys.*, *115*(A6), A06314. https://doi.org/10.1029/2009JA014563

Cui, J., Galand, M., Yelle, R. V., Wei, Y., and Zhang, S. J. (2015). Day-to-night transport in the Martian ionosphere: Implications from total electron content measurements. *J. Geophys. Res. Space Phys.*, *120*(3), 2333–2346. https://doi.org/10.1002/2014JA020788

Cui, J., Cao, Y. T., Wu, X. S., Xu, S. S., Yelle, R. V., Stone, S., Vigren, E., Edberg, N. J. T., Shen, C. L., … Wei, Y. (2019). Evaluating local ionization balance in the Nightside Martian upper atmosphere during *MAVEN* deep dip campaigns. *Astrophys. J. Lett.*, *876*(1), L12. https://doi.org/10.3847/2041-8213/ab1b34

Duru, F., Gurnett, D. A., Morgan, D. D., Winningham, J. D., Frahm, R. A., and Nagy, A. F. (2011). Nightside ionosphere of Mars studied with local electron densities: A general overview and electron density depressions. *J. Geophys. Res. Space Phys.*, *116*(A10), A10316. https://doi.org/10.1029/2011JA016835

Fowler, C. M., Andersson, L., Ergun, R. E., Morooka, M., Delory, G., Andrews, D. J., Lillis, R. J., McEnulty, T., Weber, T. D., … Jakosky, B. M. (2015). The first in situ electron temperature and density measurements of the Martian nightside ionosphere. *Geophys. Res. Lett.*, *42*(21), 8854–8861. https://doi.org/10.1002/2015GL065267

Fox, J. L., Brannon, J. F., and Porter, H. S. (1993). Upper limits to the nightside ionosphere of Mars. *Geophys. Res. Lett.*, *20*(13), 1339–1342. https://doi.org/10.1029/93GL01349

Frahm, R. A., Winningham, J. D., Sharber, J. R., Scherrer, J. R., Jeffers, S. J., Coates, A. J., Linder, D. R., Kataria, D. O., Lundin, R., … Dierker, C. (2006). Carbon dioxide photoelectron energy peaks at Mars. *Icarus*, *182*(2), 371–382. https://doi.org/10.1016/j.icarus.2006.01.014

Knudsen, W. C., Spenner, K., Miller, K. L., and Novak, V. (1980). Transport of ionospheric O^+ ions across the Venus terminator and implications. *J. Geophys. Res. Space Phys.*, *85*(A13), 7803–7810. https://doi.org/10.1029/JA085iA13p07803

Knudsen, W. C., and Miller, K. L. (1992). The Venus transterminator ion flux at solar maximum. *J. Geophys. Res. Space Phys.*, *97*(A11), 17165–17167. https://doi.org/10.1029/92JA01460

Lillis, R. J., Fillingim, M. O., Peticolas, L. M., Brain, D. A., Lin, R. P., and Bougher, S. W. (2009). Nightside ionosphere of Mars: Modeling the effects of crustal magnetic fields and electron pitch angle distributions on electron impact ionization. *J. Geophys. Res. Planets*, *114*(E11), E11009. https://doi.org/10.1029/2009JE003379

Lillis, R. J., Fillingim, M. O., and Brain, D. A. (2011). Three-dimensional structure of the Martian nightside ionosphere: Predicted rates of impact ionization from Mars Global Surveyor magnetometer and electron reflectometer measurements of precipitating electrons. *J. Geophys. Res. Space Phys.*, *116*(A12), A12317. https://doi.org/10.1029/2011JA016982

Lillis, R. J., and Brain, D. A. (2013). Nightside electron precipitation at Mars: Geographic variability and dependence on solar wind conditions. *J. Geophys. Res. Space Phys.*, *118*(6), 3546–3556. https://doi.org/10.1002/jgra.50171

Lillis, R. J., Mitchell, D. L., Steckiewicz, M., Brain, D., Xu, S. S., Weber, T., Halekas, J., Connerney, J., Espley, J., … Eparvier, F. (2018). Ionizing electrons on the Martian Nightside: structure and variability. *J. Geophys. Res. Space Phys.*, *123*(5), 4349–4363. https://doi.org/10.1029/2017JA025151

Mantas, G. P., and Hanson, W. B. (1979). Photoelectron fluxes in the Martian ionosphere. *J. Geophys. Res. Space Phys.*, *84*(A2), 369–385. https://doi.org/10.1029/JA084iA02p00369

Mitchell, D. L., Mazelle, C., Sauvaud, J. A., Thocaven, J. J., Rouzaud, J., Fedorov, A., Rouger, P., Toublanc, D., Taylor, E., … Jakosky, B. M. (2016). The MAVEN solar wind electron analyzer. *Space Sci. Rev.*, *200*(1-4), 495–528. https://doi.org/10.1007/s11214-015-0232-1

Němec, F., Morgan, D. D., Gurnett, D. A., and Duru, F. (2010). Nightside ionosphere of Mars: Radar soundings by the Mars Express spacecraft. *J. Geophys. Res. Planets*, *115*(E12), E12009. https://doi.org/10.1029/2010JE003663

Peterson, W. K., Thiemann, E., M. B., Eparvier, F. G., Andersson, L., Fowler, C. M., Larson, D., Mitchell, D., Mazelle, C., Fontenla, J., … Jakosky, B. (2016). Photoelectrons and solar ionizing radiation at Mars: Predictions versus MAVEN observations. *J. Geophys. Res. Space Phys.*, *121*(9), 8859–8870. https://doi.org/10.1002/2016JA022677

Sakai, S., Rahmati, A., Mitchell, D. L., Cravens, T. E., Bougher, S. W., Mazelle, C., Peterson, W. K., Eparvier, F. G., Fontenla, J. M., and Jakosky, B. M. (2015). Model insights into energetic photoelectrons measured at Mars by MAVEN. *Geophys. Res. Lett.*, *42*(21), 8894–8900. https://doi.org/10.1002/2015GL065169

Spenner, K., Knudsen, W. C., Whitten, R. C., Michelson, P. F., Miller, K. L., and Novak, V. (1981). On the maintenance of the Venus nightside ionosphere: Electron precipitation and plasma transport. *J. Geophys. Res. Space Phys.*, *86*(A11), 9170–9178. https://doi.org/10.1029/JA086iA11p09170

Steckiewicz, M., Mazelle, C., Garnier, P., André, N., Penou, E., Beth, A., Sauvaud, J. A., Toublanc, D., Mitchell, D. L., … Jakosky, B. M. (2015). Altitude dependence of nightside Martian suprathermal electron depletions as revealed by MAVEN observations. *Geophys. Res. Lett.*, *42*(21), 8877–8884. https://doi.org/10.1002/2015GL065257

Steckiewicz, M., Garnier, P., André, N., Mitchell, D. L., Andersson, L., Penou, E., Beth, A., Fedorov, A., Sauvaud, J. A., … Jakosky, B. M. (2017). Comparative study of the Martian suprathermal electron depletions based on Mars Global Surveyor, Mars Express, and Mars Atmosphere and volatile evolution mission observations. *J. Geophys. Res. Space Phys.*, *122*(1), 857–873. https://doi.org/10.1002/2016JA023205

Verigin, M. I., Gringauz, K. I., Shutte, N. M., Haider, S. A., Szego, K., Kiraly, P., Nagy, A. F., and Gombosi, T. I. (1991). On the possible source of the ionization in the nighttime Martian ionosphere: 1. Phobos 2 Harp electron spectrometer measurements. *J. Geophys. Res. Space Phys.*, *96*(A11), 19307–19313. https://doi.org/10.1029/91JA00924

Weber, T., Brain, D., Mitchell, D., Xu, S. S., Connerney, J., and Halekas, J. (2017). Characterization of low-altitude nightside Martian magnetic topology using electron pitch angle distributions. *J. Geophys. Res. Space Phys.*, *122*(10), 9777–9789. https://doi.org/10.1002/2017JA024491

Withers, P. (2009). A review of observed variability in the dayside ionosphere of Mars. *Adv. Space Res.*, *44*(3), 277–307. https://doi.org/10.1016/j.asr.2009.04.027

Withers, P., Fillingim, M. O., Lillis, R. J., Häusler, B., Hinson, D. P., Tyler, G. L., Pätzold, M., Peter, K., Tellmann, S., and Witasse, O. (2012). Observations of the nightside ionosphere of Mars by the Mars Express Radio Science Experiment (MaRS). *J. Geophys. Res. Space Phys.*, *117*(A12), A12307. https://doi.org/10.1029/2012JA018185

Wu, X. S., Cui, J., Yu, J., Liu, L. J., and Zhou, Z. J. (2019). Photoelectron balance in the dayside Martian upper atmosphere. *Earth Planet. Phys.*, *3*(5), 373–379. https://doi.org/10.26464/epp2019038

Xu, S. S., Mitchell, D., Liemohn, M., Dong, C. F., Bougher, S., Fillingim, M., Lillis, R., McFadden, J., Mazelle, C., … Jakosky, B. (2016). Deep nightside photoelectron observations by MAVEN SWEA: Implications for Martian northern hemispheric magnetic topology and nightside ionosphere source. *Geophys. Res. Lett.*, *43*(17), 8876–8884. https://doi.org/10.1002/2016GL070527

Xu, S. S., Mitchell, D., Liemohn, M., Fang, X. H., Ma, Y. J., Luhmann, J., Brain, D., Steckiewicz, Mazelle, M., … Jakosky, B. (2017a). Martian low-altitude magnetic topology deduced from MAVEN/SWEA observations. *J. Geophys. Res. Space Phys.*, *122*(2), 1831–1852. https://doi.org/10.1002/2016JA023467

Xu, S. S., Mitchell, D., Luhmann, J., Ma, Y. J., Fang, X. H., Harada, Y., Hara, T., Brain, D., Weber, T., … DiBraccio, G. A. (2017b). High-altitude closed magnetic loops at mars observed by MAVEN. *Geophys. Res. Lett.*, *44*(22), 11229–11238. https://doi.org/10.1002/2017GL075831

Xu, S. S., Weber, T., Mitchell, D. L., Brain, D. A., Mazelle, C., DiBraccio, G. A., and Espley, J. (2019). A technique to infer magnetic topology at mars and its application to the terminator region. *J. Geophys. Res. Space Phys.*, *124*(3), 1823–1842. https://doi.org/10.1029/2018JA026366

Zhang, M. H. G., Luhmann, J. G., and Kliore, A. J. (1990). An observational study of the nightside ionospheres of Mars and Venus with radio occultation methods. *J. Geophys. Res. Space Phys.*, *95*(A10), 17095–17102. https://doi.org/10.1029/JA095iA10p17095